Article:
Cammarano, D, Rötter, RP, Asseng, S et al. (2016) Uncertainty of wheat water use: Simulated patterns and sensitivity to temperature and CO_2. Field Crops Research, 198. pp. 80-92. ISSN: 0378-4290

https://doi.org/10.1016/j.fcr.2016.08.015

Uncertainty of wheat water use: simulated patterns and sensitivity to temperature and CO_2

Davide Cammarano[1,*], Reimund P. Rötter[2], Senthold Asseng[1], Frank Ewert[3], Daniel Wallach[4], Pierre Martre[5,6,$], Jerry L. Hatfield[7], James W. Jones[1], Cynthia Rosenzweig[8], Alex C. Ruane[8], Kenneth J. Boote[1], Peter J. Thorburn[9], Kurt Christian Kersebaum[10], Pramod K. Aggarwal[11], Carlos Angulo[3], Bruno Basso[12], Patrick Bertuzzi[13], Christian Biernath[14], Nadine Brisson[15,16,#], Andrew J. Challinor[17,18], Jordi Doltra[19], Sebastian Gayler[20], Richie Goldberg[8], Lee Heng[21], Josh E. Hooker[22,23], Leslie A. Hunt[24], Joachim Ingwersen[25], Roberto C. Izaurralde[26,26], Christoph Müller[28], Soora Naresh Kumar[29], Claas Nendel[10], Garry O'Leary[30], Jørgen E. Olesen[31], Tom M. Osborne[32], Taru Palosuo[2], Eckart Priesack[14], Dominique Ripoche[l3], Mikhail A. Semenov[33], Iurii Shcherbak[12], Pasquale Steduto[34], Claudio O. Stöckle[35], Pierre Stratonovitch[33], Thilo Streck[25], Iwan Supit[36], Fulu Tao[2, 37], Maria Travasso[38], Katharina Waha[28,^], Jeffrey W. White[39], and Joost Wolf[40]

[1]Agricultural & Biological Engineering Department, University of Florida, Gainesville, FL 32611; [2]Climate Impacts Group, Natural Resources Institute Finland (Luke), FI-00790 Helsinki, Finland; [3]Institute of Crop Science and Resource Conservation (INRES), Universität Bonn, 53115, Germany; [4]National Institute for Agricultural Research (INRA), UMR1248 Agrosystèmes et développement territorial, 31326 Castanet-Tolosan Cedex, France; [5]INRA, UMR1095 Genetics, Diversity and Ecophysiology of Cereals (GDEC), F-63 100 Clermont-Ferrand, France; [6]Blaise Pascal University, UMR1095 GDEC, F-63 170 Aubière, France; [7]National Laboratory for Agriculture and Environment, Ames, IA 50011; [8]National Aeronautics and Space Administration (NASA), Goddard Institute for Space Studies, New York, NY 10025; [9]Commonwealth Scientific and Industrial Research Organization (CSIRO), Ecosystem Sciences, Dutton Park QLD 4102, Australia; [10]Institute of Landscape Systems Analysis, Leibniz Centre for Agricultural Landscape Research, 15374 Müncheberg, Germany; [11]Consultative Group on International Agricultural Research, Research Program on Climate Change, Agriculture and Food Security, International Water Management Institute, New Delhi-110012, India;

[12]Department of Geological Sciences and Kellogg Biological Station, Michigan State University, East Lansing, MI; [13]National Institute for Agricultural Research (INRA), US1116 AgroClim, F-84 914 Avignon, France; [14]Institute of Soil Ecology, Helmholtz Zentrum München, German Research Center for Environmental Health, Neuherberg, D-85764, Germany; [15]National Institute for Agricultural Research (INRA), UMR0211 Agronomie, F-78750 Thiverval-Grignon, France; [16]AgroParisTech, UMR0211 Agronomie, F-78750 Thiverval-Grignon, France; [17]Institute for Climate and Atmospheric Science, School of Earth and Environment, University of Leeds, Leeds LS29JT, UK; [18]CGIAR-ESSP Program on Climate Change, Agriculture and Food Security, International Centre for Tropical Agriculture (CIAT), A.A. 6713, Cali, Colombia; [19]Cantabrian Agricultural Research and Training Centre (CIFA), 39600 Muriedas, Spain; [20]Water & Earth System Science Competence Cluster, c/o University of Tübingen, 72074 Tübingen, Germany; [21]International Atomic Energy Agency, 1400 Vienna, Austria; [22]School of Agriculture, Policy and Development, University of Reading, RG6 6AR, United Kingdom; [23]Joint Research Center, via Enrico Fermi, 2749 Ispra, 21027 Italy; [24]Department of Plant Agriculture, University of Guelph, Guelph, Ontario, Canada, N1G 2W1; [25]Institute of Soil Science and Land Evaluation, Universität Hohenheim, 70599 Stuttgart, Germany; [26]Dept. of Geographical Sciences, Univ. of Maryland, College Park, MD 20742; [27]Texas A&M AgriLife Research and Extension Center, Texas A&M Univ., Temple, TX 76502; [28]Potsdam Institute for Climate Impact Research, 14473 Potsdam, Germany; [29]Centre for Environment Science and Climate Resilient Agriculture, Indian Agricultural Research Institute, New Delhi 110 012, India; [30]Landscape & Water Sciences, Department of Primary Industries, Horsham 3400, Australia; [31]Department of Agroecology, Aarhus University, 8830, Tjele, Denmark; [32]National Centre for Atmospheric Science, Department of Meteorology, University of Reading, RG6 6BB, United Kingdom; [33]Computational and Systems Biology Department, Rothamsted Research, Harpenden, Herts, AL5 2JQ, United Kingdom; [34]Food and Agriculture Organization of the United Nations (FAO), Rome, Italy; [35]Biological Systems Engineering, Washington State University, Pullman, WA 99164-6120; [36]Earth System Science-CALM, Wageningen University, 6700AA, The Netherlands; [37]Institute of Geographical Sciences and Natural Resources Research, Chinese Academy of Science, Beijing 100101, China; [38]Institute for Climate and Water, INTA-CIRN, 1712 Castelar, Argentina; [39]Arid-Land Agricultural Research Center, USDA-ARS, Maricopa,

AZ 85138; [40]Plant Production Systems, Wageningen University, 6700AA Wageningen, The Netherlands.

[*] Present address: James Hutton Institute, Invergowrie, Dundee, DD2 5DA, Scotland, UK

[$] *Present address*: INRA, Montpellier SupAgro, UMR759 Laboratoire d'Ecophysiologie des Plantes sous Stress Environnementaux, F-34 060 Montpellier, France

[^] *Present address*: Commonwealth Scientific and Industrial Research Organization (CSIRO), Agriculture, 306 Carmody Road, 4067 St.Lucia, Australia

Corresponding author:
Davide Cammarano
Agricultural & Biological Engineering Department, University of Florida, Gainesville, FL, 32611, U.S.A.
Phone: +1 352-392-1864 ext.237; E-mail: davide.cammarano@ufl.edu
Present Address: The James Hutton Institute, Invergowrie, Dundee, DD2 5DA, U.K.
Phone: +44 (0) 844 928 5428; E-mail: Davide.Cammarano@hutton.ac.uk

Abstract

Projected global warming and population growth will reduce future water availability for agriculture. Thus, it is essential to increase the efficiency in using water to ensure crop productivity. Quantifying crop water use (WU; i.e. actual evapotranspiration) is a critical step towards this goal. Here, sixteen wheat simulation models were used to quantify sources of model uncertainty and to estimate the relative changes and variability between models for simulated WU, water use efficiency (WUE, WU per unit of grain dry mass produced), transpiration efficiency (T_{eff}, transpiration per kg of unit of grain yield dry mass produced), grain yield, crop transpiration and soil evaporation at increased temperatures and elevated atmospheric carbon dioxide concentrations ([CO_2]). The greatest uncertainty in simulating water use, potential evapotranspiration, crop transpiration and soil evaporation was due to differences in how crop transpiration was modelled and accounted for 50% of the total variability among models. The simulation results for the sensitivity to temperature indicated that crop WU will decline with increasing temperature due to reduced growing seasons. The uncertainties in simulated crop WU, and in particularly due to uncertainties in simulating crop transpiration, were greater under conditions of increased temperatures and with high temperatures in combination with elevated atmospheric [CO_2] concentrations. Hence the simulation of crop WU, and in particularly crop transpiration under higher temperature, needs to be improved and evaluated with field measurements before models can be used to simulate climate change impacts on future crop water demand.

Keywords: multi-model simulation; transpiration efficiency; water use; uncertainty; sensitivity.

1. Introduction

Globally, agriculture uses about 70% of all freshwater withdrawals for irrigation, although discrepancies exist in the quantified amount (Alcamo et al., 2007; Howell, 2001; Shen et al., 2008). About 70% of the world's wheat production comes from irrigated or high rainfall regions, with the majority of irrigation concentrated in developing countries with high population density, particularly large producers like China and India (Dixon et al., 2009; Reynolds and Braun, 2013). Projections that global food demand will double by 2050 highlight the challenges agriculture is facing with the need to produce more food with less land and less water (Foley et al., 2011; Godfray et al., 2010). Due to continued population growth, urbanization and industrialization, agriculture will increasingly compete with other sectors for freshwater (Godfray et al., 2010; Siebert and Doll, 2010; Tilman et al., 2011), and climate change may further limit water availability for irrigation in many cropping areas (Elliott et al., 2014). In rainfed agricultural environments, where crops rely on rainfall alone, future changes in rainfall patterns, temperature conditions, and increases in atmospheric carbon dioxide concentrations ($[CO_2]$) will affect crop production (Challinor et al., 2014; Knox et al., 2012; Müller and Robertson, 2014; Rosenzweig and Parry, 1994; Rötter and Van de Geijn, 1999).

Passioura (2006) discussed how the term "water productivity", in the context of agriculture, has different meanings to different people in terms of significance and timescale of interest. Similarly, different aspects of the water used in agriculture are of interest to different actors and stakeholders. These aspects are often characterized in terms of crop water use (WU, known also as actual evapotranspiration), water use efficiency (WUE, defined in eq. 7), and transpiration efficiency (T_{eff}, defined in eq. 8). For example, breeders use the ratio of agronomic performance

(e.g. grain yield) to cumulated WU (WUE) as a basis for identifying crop ideotypes with better productivity, agronomists use WUE as a benchmark for identifying management practices suitable for irrigated or rainfed cultivation, while farmers may be more interested in WUE from an economic point of view (e.g. the monetary outcome such as marketable yield, given a unit of input used to produce it) (Blum, 2005; Condon et al., 2002; Passioura, 2006; Passioura and Angus, 2010; Sadras and Angus, 2006; Semenov et al., 2014). The improvement of crop productivity through management and breeding for high WUE has been the subject of numerous studies (Condon et al., 2004; Condon et al., 2002; Sinclair and Muchow, 2001). Tools that extrapolate the effects of future temperature and [CO_2] changes on how WU, WUE, and T_{eff} are likely to respond can complement information from field/greenhouse-based experiments for developing guidance on suitable climate change adaptations.

Crop simulation models (CSMs) are increasingly used to explore and assess climate change impacts on agriculture (Angulo et al., 2013; Osborne et al., 2013; White et al., 2011a). CSMs can account for multiple interactions among climate, crop, soil and management. CSMs differ in the way they simulate soil-plant-atmosphere processes and in the number of parameters and inputs required (Rötter et al., 2012; White et al., 2011a). Some CSMs have been developed, evaluated and applied in specific agro-environments, and these models don't perform equally well across all environments.

Single CSMs have usually been used to assess biophysical impacts due to climate change, but it is not possible to evaluate various sources of uncertainty with a single CSM (White et al., 2011a). One method of studying uncertainties in climate models that has become common practice is to use ensembles of multiple global and regional climate models (Mearns et al., 1997; Tebaldi and Knutti, 2007). Until recently, model ensembles have seen limited use in modelling

climate change impact on agriculture (Rötter et al., 2011). Mean or median simulations from multi-model ensembles are usually more accurate than any individual model (Asseng et al., 2013; Martre et al., 2015; Rötter et al., 2012). A further benefit of ensembles is that the variability among the simulations from an ensemble can be used to estimate the uncertainty range when using different CSMs.

In this paper we used simulations from a recent multi-model study (Asseng et al., 2013) that focused solely on wheat grain yield, to explore simulations of crop WU, WUE, and T_{eff} and their variability and sensitivity to temperature and [CO_2] changes.

The objectives of this study were to: i) quantify the contributions of sources of model uncertainty to calculations of crop transpiration, soil evaporation, and potential evapotranspiration; and to ii) estimate the relative changes, the patterns and the variability between models for the simulated WU, WUE, T_{eff}, yield, crop transpiration and soil evaporation at elevated temperatures and [CO_2].

2. Materials and methods

2.1 Experimental sites

Experimental data from four locations with contrasting growing season rainfall and temperature were used which were described in details in Asseng et al. (2013). The locations were Wageningen–NL (Groot et al., 1991), Balcarce – AR (Travasso et al., 1995), New Delhi – IN (Naveen, 1986), and Wongan Hills – AU (Asseng et al., 1998). In particular, the experimental sites were defined in terms of yield and season length as high yielding and long season in the NL, high/medium yielding and medium season in AR, irrigated and short season in IN, and low

yielding, rainfed, short season in AU (Asseng et al., 2013). These locations were chosen to represent four different wheat mega-environments, a concept used by wheat breeders for testing cultivars (Monfreda et al., 2008) that accounts for about 80% of the wheat-growing area of the world (Additional details were provided in Tables S1 and S2).

The data were quality controlled and standardized using the AgMIP data protocols (Rosenzweig et al., 2011). The management information used at each site was obtained from the experimentalists. The crops were kept weed and disease-free. Daily weather data of solar radiation, maximum and minimum temperature and rainfall were recorded at weather stations on site, with the exception of IN, where solar radiation was obtained from the NASA POWER dataset (White et al., 2011b). At NL, the average daily wind speed at 2-meter height was measured. At the three other locations daily wind speed was estimated using the NASA Modern Era Retrospective-Analysis for Research and Applications (MERRA) (Rienecker et al., 2011). At all locations dew-point temperature was estimated using MERRA. Atmospheric [CO_2] was assumed to be at 360 ppm for all the locations, in line with measured atmospheric [CO_2] for the mid-point (year 1995) of the baseline climate period 1980-2009.

Measured experimental field data used for this study were harvested grain dry matter yield (Y, t ha^{-1}), in-season measurements of total aboveground biomass (dry matter) (AGB; t ha^{-1}), leaf area index (LAI, m^2 m^{-2}), water use (WU, mm), and soil water content to maximum rooting depth (SWC, Vol%). For each location soil the soil layers were supplied to all modelling groups (Table S2). For each soil layer (i for up to n layers) and from the layer-specific SWC, the plant available soil water content to maximum rooting depth (PAW, mm) was calculated using the lower limit of water extraction for each soil layer (LL, Vol%) which is similar to the soil moisture content at wilting point, and the thickness of each soil layer (st, m) as follows:

$$PAW = \sum_{i=1}^{n} st_i * (SWC_i - LL_i) \quad [1]$$

At NL, the SWC was measured down to 1 m, so the SWC and PAW were calculated assuming that the soil between 1 m and maximum rooting depth of 2 m was similar to the 0.6-1 m layers. At AR, the SWC was measured down to 1.2 m and the maximum rooting depth was 1.3 m. While, in IN and AU the SWC was measured up to 1.5 m and 2.1m, and the maximum rooting depth was 160 and 210, respectively.

Soil water balance (SWB) was calculated for each simulation run using the simulated drainage (mm), runoff (mm), crop transpiration (mm), soil evaporation (mm), and rainfall (mm) for NL, AR, AU, while for IN irrigation was also considered (mm). To calculate the ΔSoil Water Change (SWB) the following equation was used:

SWB = Rain + Irrigation – Drainage – Runoff – Transpiration – Evaporation [2]

2.2 Crop Models

Based on a twenty-six member multi-model ensemble study conducted by Asseng et al. (2013), sixteen crop models which simulate crop transpiration (*Ta*) and soil evaporation (*Es*) as separate fluxes were selected for detailed analysis of water use simulations (for more detailed information on the simulated processes see Table S3). The models, which varied in complexity and functionalities, have all been described and used in modelling wheat crops. Additional details on modelling procedures were described in Asseng et al. (2013), for this study we used the models calibrated against phenology and yield. At the beginning of the study a questionnaire was sent to the modelers to provide information on which type of ET_0 was used in the crop models. Information on different implementations of the ET_0 calculation in the 16 wheat models

using the Penman (P; Penman, 1948), Penman-Monteith (PM; Allen et al., 1998) or Priestley-Taylor (PT; Priestly and Taylor, 1972) equations (Tab. S3). Analysis of variance (ANOVA) for unbalanced designs was used to test the differences among the three ET_0 formulas at each location.

2.4 Data analysis

The partitioning of uncertainty of simulated WU was made to explore which component was responsible for most of the variability. WU can be expressed as follows, based on simulated cumulative ΣET_0, ΣTa and ΣEs:

$$\mathrm{WU} = \sum ETo * \left[\frac{\sum Es}{\sum ETo} + \frac{\sum Ta}{\sum ETo}\right] \quad [3]$$

The variance is calculated as follows:

$$Var(\mathrm{WU}) = Var\left(\frac{\sum Ta}{\sum ETo}\right) * E(\sum ETo)^2 + Var\left(\frac{\sum Es}{\sum ETo}\right) * E(\sum ETo)^2 + Var(\sum ETo) * \left[E\left(\frac{\sum Es}{\sum ETo} + \frac{Ta}{\sum ETo}\right)\right]^2 \quad [4]$$

where $\sum Ta / \sum ETo$ was transpiration as a fraction of evaporative demand and $\sum Es / \sum ETo$ was soil evaporation as a fraction of evaporative demand. A way of quantifying the contribution of $\sum Ta / \sum ETo$, $\sum Es / \sum ETo$, and ΣET_0 to the overall uncertainty was through the first-order sensitivity coefficients (S1):

$$S1(Ta) = Var(\sum Ta / \sum ETo) * E(\sum ETo)^2 \quad [5]$$

$$S1(Es) = Var(\sum Es / \sum ETo) * E(\sum ETo)^2 \quad [6]$$

$$S1(ETo) = Var(\sum ETo) * [E(\sum Es / \sum ETo + \sum Ta / \sum ETo)]^2 \quad [7]$$

If there are no interactions among terms, S1(x) is the fraction of overall variance contributed by factor x and the sum of the S1 can be somewhat larger or smaller than 1, depending on whether there were positive or negative correlations between terms. The larger the values of S1(x), the greater the contribution of factor x to the overall variance. From the sum of the first-order sensitivity coefficients, we calculated the percentage contribution of each term.

Water use efficiency (WUE) was calculated as:

$$\mathrm{WUE} = \frac{Y}{\Sigma \mathrm{WU}} \quad [8]$$

where Y is the simulated grain dry matter yield and ΣWU was the cumulative evapotranspiration calculated from sowing to harvest. Transpiration efficiency (T_{eff}) on a grain yield basis was calculated following the definition of Angus and van Herwaarden (2001):

$$T_{\mathrm{eff}} = \frac{Y}{\sum Ta} \quad [9]$$

where ΣTa is the cumulative water transpired from sowing to harvest.

2.5 Sensitivity analysis

In addition to the simulations based on the measured experimental conditions, simulations were conducted using daily weather data for the period 1980-2010 for all the locations to create a baseline. A sensitivity analysis of the sixteen models to temperature and [CO_2] was done using a partly-factorial design. Daily minimum and maximum temperature were increased by either 3°C (+3C) or 6°C (+6C) and [CO_2] was increased in 90 ppm increments from a baseline to a maximum of 720 ppm. Wind speed and relative humidity were kept unchanged with the increased temperatures, so vapor pressure was re-calculated using the modified temperatures. In

order to understand the effects of climate factors alone on crop responses, soil and crop management were kept the same for all the simulations except that dates of irrigation and fertilization were adapted to the changed phenology.

The relative changes in *Y*, WU, *Ta*, *Es*, WUE, and T_{eff} were calculated as:

$$r_k = \frac{\bar{y}_{sensitivity,k} - \bar{y}_{baseline,k}}{\bar{y}_{baseline,k}} * 100 \quad [10]$$

where r_k is the predicted relative change with respect to the 30-year baseline according to model *k*, $\bar{y}_{sensitivity,k}$ is any of the above variables averaged over the 30 years of climate sensitivity according to model *k*, and $\bar{y}_{baseline,k}$ are the variables averaged over the 30 years of baseline climate according to model *k*.

More detailed analysis of the multi-model intercomparison in terms of decomposition of the mean square error and other statistical indicators can be found in Martre et al. (2015).

3. Results

3.1 Decomposition of the variability

The simulated growing season ET_0 using the three methods (PM, PT, and P) ranged from 786 mm for AU to 483 mm for the NL (Fig. 1a). Total season ET_0 values calculated by the three methods differed at each location ($P < 0.05$; Fig. 1a).

When the uncertainty of simulated WU was partitioned between *Ta, Es,* and ET_0, and following equations [2] to [6], the first-order sensitivity coefficient S1(*Ta*) contributed the most to the variability in WU among models (Fig. 1b-d). For the single year dataset the term S1(*Ta*) was 46% of the variability, S1(*Es*) was 30%, and (ET_0) was 24% (Fig. 1b). For the simulations

averaged over the 30-year baseline, S1(*Ta*), S1(*Es*), and S1(ET_0) were 51%, 28% and 21%, respectively (Fig. 1b). There was little change in the first order sensitivity coefficients as temperature increased. The S1(*Ta*), S1(*Es*), and S1(ET_0) values were 46, 37, and 18% at +3C and 50, 36 and 14% at +6C (Fig. 1c). Simulations with four [CO_2] showed similar results with S1(*Ta*) ranging between 53 and 54% (Fig. 1d).

3.2 Observed and simulated data

The daily patterns of growing season rainfall, observed and simulated PAW, ET_0, LAI, E*s*, T*a*, WU, and AGB are shown for NL, AR, IN, and AU in Figs. 2-5, respectively. The four wheat-growing locations differed in terms of the evaporative demand of the atmosphere, soil conditions, and the temporal variability of growing season rainfall and temperature (Figs. 2-5). For example, at AU rainfall occurred frequently throughout the season with occasional days of heavy rainfall in spring and summer (Fig. 5a). In contrast, there was no rainfall at the IN site (Fig. 4a). NL and AR had frequent heavy rainfall during the growing season (Figs. 2a and 3a). The in-season observed values for the plant available soil water, aboveground biomass, water use, and LAI were within the range of the simulations in NL, AR, and AU (Figs. 2,3, and 5). There were some discrepancies between observed and simulated values in IN for the LAI, PAW and WU (Fig. 4).

The end-of-season cumulative WU, WUE, *Ta*, *Es*, T_{eff}, and *Y* for the single experimental year, and for the 30-year period from 1980 to 2009 are shown in Table 1. Simulated average values for WU was less variable than for WUE and T_{eff}. The coefficient of variation (CV) across locations for the single experimental year varied between 14 and 23% for WU, and between 16 and 37%

for WUE. Average CV of simulated values varied between 20 and 33% for *Ta*, between 34 and 73% for *Es*, and between 24 and 55% for T_{eff} (Table 1).

3.3 Crop simulation models sensitivity to average daily air temperature and atmospheric CO_2 concentration

The average simulated WU, *Y*, *Ta*, *Es*, WUE, and T_{eff} decreased with increased temperature for all four locations (Fig. 6). However, the variability of the models increased as temperature increased for all the variables (Fig. 6). The models showed higher uncertainties for Australia, where except for the simulated WU which had little variability. In Australia simulated T_{eff} varied between -100 and +100% when temperature was increased by +6C (Fig. 6).

Simulated average WU, *Ta*, and *Es* decreased with increasing [CO_2] while Y, WUE, and T_{eff} increased with increasing [CO_2] at all locations (Fig. 7). The simulated relative changes to [CO_2] showed less variability than temperature. This outcome seemed to be consistent across the models, with the exception of few outliers. At 720 compared to 360 ppm [CO_2] in the four locations, the overall simulated values changed by -4% for WU, +31% for *Y*, -2% for *Ta*, -9% for *Es*, +38% for WUE, and +34% for T_{eff} (Fig. 7). Only the variability of WUE and Teff was higher at 720 ppm than at 360 ppm, ranging between 0 and 100% changes at 720 ppm (Fig. 7).

The respective effects of changing temperature and [CO_2] interact in generating model outputs of the 16 crop models. For simulated *WU*, increasing [CO_2] to 720 ppm does not offset its reduction caused by temperature increase (Figure 8). The effects of [CO_2] in compensating temperature-induced losses of WUE and T_{eff} were larger than for simulated *WU* (Fig. 8). For

example, with a 6°C increase, WUE increased if [CO_2] was above 450 ppm in NL and IN, or above 550 ppm in AR and AU (Fig. 8).

Of particular interest is the variability in the direction of change in simulated responses to increased temperature or [CO_2]. It was studied by counting how many models showed similar trend; for example how many models simulated a decrease in WU at +6C, and how many simulated an increase in WU at +6C. Overall, with a 6°C increase across the four locations, 94% of the models computed that WU decreased, 83% that *Ta* decreased, 52% that *Es* decreased, 78% that WUE decreased, and 63% that T_{eff} decreased (Fig. 6). Modelling the effect of 720 ppm CO_2, 69% of the models agreed that WU decreased, 97% that *Y* increased, 56% that *Ta* decreased, and 83% that *Es* decreased. All models projected that WUE and T_{eff} would increase (Fig. 7).

The calculated SWB using eq. [2] showed that for both baseline and sensitivity to temperature and CO_2 the NL had a higher variability among the models with respect to the other locations (Fig. 9). The variability among the different components of eq. [2] showed that transpiration (Ta) was the component having the higher variability followed by the drainage (Fig. 10). For example, in the NL the simulated transpiration varied between 100 and 500 mm for the baseline runs (No temperature changes) and drainage between 0 and 400 mm, for the upper and lower hinge representing the 25^{th} and 75^{th} percentile, respectively. At +6C the variability of simulated crop transpiration among models ranged between 10 and 540 mm while simulated drainage ranged between 0 and 350 mm (Fig. 10a).

4. Discussion

In this study, most of the variability in simulated WU was due to model differences in Ta/ETo and Es/ETo rather than the choice of the ET_0 formula. This is true for the experimental years, the 30-year baseline and for the simulations with increased temperature or CO_2. While differences in the choice of the ET_0 formula have been shown to be important (Kingston et al., 2009; McAfee, 2013; McKenney and Rosenberg, 1993; Utset et al., 2004; Xu and Singh, 2002), studies focusing on the ET_0 formula have not analyzed how the partitioning of ET_0 between *Es* and *Ta* would influence the simulations of crop WU. Other studies have focused on the partitioning within the growing season of the *Es* and *Ta* only, showing that *Es* can account for 20% to 40% of WU (Kool et al., 2014; French and Sculz, 1984).

Although the overall first order effect of Ta/ETo accounted for 51% of the total of first order effects on WU for both different temperature and CO_2 changes across the four locations, no experimental data were available to validate these aspects of the simulation. Differences among models in simulating rooting depth/distribution and soil water extraction by roots could be an important reason for differences in *Ta* estimation (Wu and Kersebaum, 2008).

Understanding the partitioning of WU between crop transpiration and soil evaporation is critical because of its implications for agricultural, ecological, and hydrological studies. In addition, considering the variability in the simulation of PAW, and particularly of simulated LAI, the differences in Ta/ETo are not surprising because the water is transpired by crops through stomata that are on leaves.

Given the variability of the simulated SWB, and of the other components like drainage, further research into the reasons of variation of different sub-routines among models is necessary. The hardest part is to get detailed and accurate measurements of each sub-component in a single experiment.

The large variability between models indicates that there are major differences in the way the processes that affect water use are modeled. Differences among models in simulating soil water extraction by roots could be an important reason for differences in Ta estimation (Wu and Kersebaum, 2008). Variability in the simulation of PAW and LAI would have a direct effect on the differences in Ta/ET_o. Since PAW was among the given soil parameters, causes are primarily related to differences in the models' crop interfaces to soil (roots) and atmosphere (LAI).

Models have been tested against the same limited set of CO_2 response data, which are from open-top chamber or Free Air Carbon dioxide Enrichment Experiments (FACE) data. Models also typically include many processes that respond to temperature, while the response to CO_2 is often lumped at a higher level of integration as discussed in details by Kersebaum and Nendel (2014). Some models used an empirical relationship between CO_2 and radiation use efficiency while other models used the CO_2 dependency of the photosynthesis light response curve (Tubiello and Ewert, 2002) or directly simulated stomatal conductance and rubisco-kinetics based photosynthesis.

However, there is no clear relationship between model results and model's structure because models are complex and many elements of structure interact with each other (Bassu et al., 2014; Li et al., 2015; Martre et al., 2015). Further research into the sources of variation of different sub-routines among models is necessary.

Increased [CO_2] in field crops has led to decreases in WU of 3 to 8%, and an increase in Y of 8 to 31% (Hatfield et al., 2011; Kimball et al., 2002; Long et al., 2006; Manderscheid and Weigel, 2007; Tao and Zhang, 2013). The variability in the experimental results depends on crop management, CO_2 concentrations used in the experiments, the type of experiment (e.g. open-top chambers or field experiments), and the different scaling methods used to compare a crop

response to CO_2 concentrations across different experiments (Long, 2012). A meta-analysis of wheat studies found that increasing [CO_2] from 400 to 800 ppm increases WUE by between 5 and 38% (Hatfield et al., 2011; Kimball et al., 2002; Long et al., 2006; Manderscheid and Weigel, 2007; Tao and Zhang, 2013; Wang et al., 2013). The results of this study regarding the simulated response at the four locations for WU, *Y*, and WUE to [CO_2] was in line with these studies. This concordance contrasts with claims that on average models overestimate [CO_2] effects (Ewert et al., 2007; Long et al., 2006; Tubiello et al., 2007).

Another important outcome of our study is to have traced the average pattern of WU, WUE, and T_{eff} change with temperature and [CO_2] increases. Despite variability, the majority of models had the same direction of change in *Y*, WU, WUE, and T_{eff} in the sensitivity to temperature and [CO_2]. This allowed us to draw conclusions about general crop responses when temperature and [CO_2] both change. The interaction between increase in temperature and increase in [CO_2] showed that, depending on the location, *Y*, WUE, and T_{eff} reductions due to temperature can be largely offset by increasing [CO_2]. The response of WUE to temperature is of particular interest since this response may be driving yield changes in many regions with limited rainfall and water for irrigation (Pirttioja et al., 2015).

The changes in temperature used in this study (+3°C and +6°C) caused more model output variability than the changes in atmospheric [CO_2] (from 360 ppm to 720 ppm at 90 ppm intervals). But, the crop models' agreement related to the magnitude of changes is variable-specific. For example, crop models showed good agreement in terms of relative change of simulated Y under temperature and elevated [CO_2] changes, WU showed good agreement under temperature changes and lower agreement under [CO_2], while WUE, and T_{eff} showed less agreement under temperature changes and high agreement under elevated [CO_2] (Fig. 6 and 7).

5. Conclusion

The largest uncertainty in simulated crop WU among CSMs is due to differences in how models simulate crop transpiration. The simulated response to increased temperature caused a decline in WU. The sixteen models showed greatest uncertainty of simulated WUE, and T_{eff} at increased temperatures and with interactions between temperature and [CO_2]. To improve the simulated impacts of climate change on crop water dynamics, crop transpiration in CSMs needs to be improved with detailed experimental data.

Acknowledgments

We thank the anonymous referees for the valuable comments and suggestions that helped improve the manuscript.

S.G. was supported by a grant from the Ministry of Science, Research and Arts of Baden-Württemberg (AZ Zu 33-721.3-2) and the Helmholtz Center for Environmental Research, Leipzig (UFZ); R.P.R., T.P. and F.T. were supported by funds from the European FACCE MACSUR project through the Finnish Ministry of Agriculture and Forestry; P.M., P.B., N.B. and D.R. were supported by INRA Environment and Agronomy Division and by the funding within the framework of JPI FACCE MACSUR project through the INRA Metaprogram on the Adaptation of Agriculture and Forests to Climate Change; K.C.K. and C.N. received support from the German Federal Office for Agriculture and Food with FACCE MACSUR (2812ERA147) and from COST ES1106; C.M. acknowledges financial support from the KULUNDA project (01LL0905L) and the FACCE MACSUR project (031A103B) funded

through the German Federal Ministry of Education and Research (BMBF); C.O.S. was supported by the project of Regional Approaches to Climate Change for Pacific Northwest Agriculture (REACCH-PNA) funded through award #2011-68002-30191 from the National Institute for Food and Agriculture.

Reference

Alcamo, J., Florke, M. and Marker, M., 2007. Future long-term changes in global water resources driven by socio-economic and climatic changes. Hydrolog Sci J, 52(2): 247-275.

Allen, R.G., Pereira, L.S., Raes, D. and Smith, M., 1998. Crop evapotranspiration: guidelines for computing crop water requirements - FAO irrigation and drainage paper 56. FAO, via Terme di Caracalla, Rome.

Angulo, C. et al., 2013. Implication of crop model calibration strategies for assessing regional impacts of climate change in Europe. Agr Forest Meteorol, 170: 32-46.

Angus, J.F. and van Herwaarden, A.F., 2001. Increasing water use and water use efficiency in dryland wheat. Agronomy Journal, 93(2): 290-298

Asseng, S. et al., 2013. Uncertainty in simulating wheat yields under climate change. Nature Climate Change, 3(9): 827-832.

Asseng, S. et al., 1998. Performance of the APSIM-wheat model in Western Australia. Field Crops Research, 57(2): 163-179.

Bassu, S. et al., 2014. How do various maize crop models vary in their responses to climate change factors? Global Change Biology, 20(7): 2301-2320.

Blum, A., 2005. Drought resistance, water-use efficiency, and yield potential - are they compatible, dissonant, or mutually exclusive? Australian Journal of Agricultural Research, 56(11): 1159-1168.

Brisson, N., Itier, B., L'Hotel, J.C. and Lorendeau, J.Y., 1998. Parameterisation of the Shuttleworth-Wallace model to estimate daily maximum transpiration for use in crop models. Ecological Modelling, 107(2-3): 159-169.

Challinor, A.J. et al., 2014. A meta-analysis of crop yield under climate change and adaptation. Nat Clim Change, 4(4): 287-291.

Condon, A., Richards, R., Rebetzke, G. and Farquhar, G., 2004. Breeding for high water-use efficiency. Journal of Experimental Botany, 55(407): 2447-2460.

Condon, A.G., Richards, R.A., Rebetzke, G.J. and Farquhar, G.D., 2002. Improving intrinsic water-use efficiency and crop yield. Crop Science, 42(1): 122-131.

Dixon, J., Braun, H.J. and Crouch, J., 2009. Overview: Transitioning Wheat Research to Serve the Future Needs of the Developing World In: J. Dixon, H.J. Braun, P. Kosina and J. Crouch (Editors), Wheat Facts and Futures 2009. CIMMYT, Mexico, D.F.

Elliott, J. et al., 2014. Constraints and potentials of future irrigation water availability on agricultural production under climate change. P Natl Acad Sci USA, 111(9): 3239-3244.

Ewert, F., Porter, J.R. and Rounsevell, M.D.A., 2007. Crop models, CO2, and climate change. Science, 315(5811): 459-459.

Foley, J.A. et al., 2011. Solutions for a cultivated planet. Nature, 478: 337-342.

French, R.J., Schultz, J.E., 1984. Water use efficiency of wheat in a Mediterranean-type environment. I the relationship between yield, water use and climate. Australian Journal of Agricultural Research, 35: 743–764.

Godfray, H.C.J. et al., 2010. Food Security: The Challenge of Feeding 9 Billion People. Science, 327(5967): 812-818.

Groot, J.J.R., De Willigen, P. and Verberne, E.L.J., 1991. Nitrogen turnover in the soil-crop system. Developments in Plant and Soil Sciences, 44. Kluver Academic Publisher, Haren.

Hansen, S., 1984. Estimation of potential and actual evapotranspiration. Nordic Hydrology, 15(4-5): 205-212.

Hatfield, J.L. et al., 2011. Climate Impacts on Agriculture: Implications for Crop Production. Agronomy Journal, 103(2): 351-370.

Howell, T.A., 2001. Enhancing water use efficiency in irrigated agriculture. Agronomy Journal, 93(2): 281-289.

Kersebaum, K.C. and Nendel, C., 2014. Site-specific impacts of climate change on wheat production across regions of Germany using different CO2 response functions. European Journal of Agronomy, 52: 22-32.

Kimball, B.A., Kobayashi, K. and Bindi, M., 2002. Responses of agricultural crops to free-air CO2 enrichment. Advances in Agronomy, Vol 77, 77: 293-368.

Kingston, D.G., Todd, M.C., Taylor, R.G., Thompson, J.R. and Arnell, N.W., 2009. Uncertainty in the estimation of potential evapotranspiration under climate change. Geophys Res Lett, 36.

Knox, J., Hess, T., Daccache, A. and Wheeler, T., 2012. Climate change impacts on crop productivity in Africa and South Asia. Environ Res Lett, 7(3).

Kool, D. et al., 2014. A review of approaches for evapotranspiration partitioning. Agricultural and Forest Meteorology, 184: 56-70.

Li, T. et al., 2015. Uncertainties in predicting rice yield by current crop models under a wide range of climatic conditions. Global Change Biology, 21(3): 1328-1341.

Long, S.P., 2012. Virtual Special Issue on food security - greater than anticipated impacts of near-term global atmospheric change on rice and wheat. Global Change Biol, 18(5): 1489-1490.

Long, S.P., Ainsworth, E.A., Leakey, A.D.B., Nosberger, J. and Ort, D.R., 2006. Food for thought: Lower-than-expected crop yield stimulation with rising CO2 concentrations. Science, 312(5782): 1918-1921.

Manderscheid, R. and Weigel, H.J., 2007. Drought stress effects on wheat are mitigated by atmospheric CO2 enrichment. Agron Sustain Dev, 27(2): 79-87.

Martre, P. et al., 2015. Multimodel ensembles of wheat growth: many models are better than one. Global Change Biology, 21(2): 911-925.

McAfee, S.A., 2013. Methodological differences in projected potential evapotranspiration. Climatic Change, 120(4): 915-930.

McKenney, M.S. and Rosenberg, N.J., 1993. Sensitivity of some potential evapotranspiration estimation methods to climate change. Agricultural and Forest Meteorology, 64(1-2): 81-110.

Mearns, L.O., Rosenzweig, C. and Goldberg, R., 1997. Mean and variance change in climate scenarios: Methods, agricultural applications, and measures of uncertainty. Climatic Change, 35(4): 367-396.

Monfreda, C., Ramankutty, N. and Foley, J.A., 2008. Farming the planet: 2. Geographic distribution of crop areas, yields, physiological types, and net primary production in the year 2000. Global Biogeochem Cy, 22(1).

Müller, C. and Robertson, R.D., 2014. Projecting future crop productivity for global economic modeling. Agricultural Economics, 45(1): 37-50.

Naveen, N., 1986. Evaluation of soil water status, plant growth and canopy environemtn in relation to variable water supply to wheat, Indian Agricultural Research Institute, New Delhi, India.

Osborne, T., Rose, G. and Wheeler, T., 2013. Variation in the global-scale impacts of climate change on crop productivity due to climate model uncertainty and adaptation. Agr Forest Meteorol, 170: 183-194.

Palosuo, T. et al., 2011. Simulation of winter wheat yield and its variability in different climates of Europe: A comparison of eight crop growth models. European Journal of Agronomy, 35(3): 103-114.

Passioura, J., 2006. Increasing crop productivity when water is scarce - from breeding to field management. Agricultural Water Management, 80(1-3): 176-196.

Passioura, J.B. and Angus, J.F., 2010. Improving productivity of crops in water-limited environments. Advances in Agronomy, Vol 106, 106: 37-75.

Penman, H.L., 1948. Natural Evaporation from Open Water, Bare Soil and Grass. Proc R Soc Lon Ser-A, 193(1032): 120-&.

105 Pirttioja, N., Carter, T.R., Fronzek, S., 2015. A crop model ensemble analysis of temperature and
106 precipitation effects on wheat yield across a European transect using impact response
107 surfaces. Climate Research, 65: 87–105.

108 Priestley, C. and Taylor, R.J., 1972. On the assessment of surface heat flux and evaporation
109 using large scale parameters. Monthly Weather Review, 100(2): 10.

110 Reynolds, M. and Braun, H., 2013. Achieving yield gains in wheat: Overview. In: M. Reynolds
111 and H. Braun (Editors), Proceedings of the 3rd International Workshop of the Wheat
112 Yield Consortium. CIMMYT, Obregón, Sonora, Mexico.

113 Rienecker, M.M. et al., 2011. MERRA: NASA's Modern-Era Retrospective Analysis for
114 Research and Applications. J Climate, 24(14): 3624-3648.

115 Rosenzweig, C., Jones, J.W., Hatfield, J. and Antle, J., 2011. AgMIP Protocols
116 http://www.agmip.org/agmip-protocols/, accessed July 2014.

117 Rosenzweig, C. and Parry, M.L., 1994. Potential Impact of Climate-Change on World Food-
118 Supply. Nature, 367(6459): 133-138.

119 Rötter, R. and Van de Geijn, S.C., 1999. Climate change effects on plant growth, crop yield and
120 livestock. Climatic Change, 43(4): 651-681.

121 Rötter, R.P., Carter, T.R., Olesen, J.E. and Porter, J.R., 2011. Crop-climate models need an
122 overhaul. Nat Clim Change, 1(4): 175-177.

123 Rötter, R.P. et al., 2012. Simulation of spring barley yield in different climatic zones of Northern
124 and Central Europe: A comparison of nine crop models. Field Crop Res, 133: 23-36.

125 Sadras, V.O. and Angus, J.F., 2006. Benchmarking water-use efficiency of rainfed wheat in dry
126 environments. Aust J Agr Res, 57(8): 847-856.

127 Semenov, M.A., Stratonovitch, P., Alghabari, F. and Gooding, M.J., 2014. Adapting wheat in
128 Europe for climate change. J Cereal Sci, 59(3): 245-256.

129 Shen, Y.J., Ok, T., Utsumi, N., Kanae, S. and Hanasaki, N., 2008. Projection of future world
130 water resources under SRES scenarios: water withdrawal. Hydrolog Sci J, 53(1): 11-33.

131 Siebert, S. and Doll, P., 2010. Quantifying blue and green virtual water contents in global crop
132 production as well as potential production losses without irrigation. J Hydrol, 384(3-4):
133 198-217.

134 Sinclair, T.R. and Muchow, R.C., 2001. System analysis of plant traits to increase grain yield on
135 limited water supplies. Agronomy Journal, 93(2): 263-270.

136 Tao, F.L. and Zhang, Z., 2013. Climate change, wheat productivity and water use in the North
137 China Plain: A new super-ensemble-based probabilistic projection. Agr Forest Meteorol,
138 170: 146-165.

139 Taylor, S.L., Payton, M.E. and Raun, W.R., 1999. Relationship between mean yield, coefficient
140 of variation, mean square error, and plot size in wheat field experiments. Commun Soil
141 Sci Plan, 30(9-10): 1439-1447.

142 Tebaldi, C. and Knutti, R., 2007. The use of the multi-model ensemble in probabilistic climate
143 projections. Philos T R Soc A, 365(1857): 2053-2075.

144 Tilman, D., Balzer, C., Hill, J. and Befort, B.L., 2011. Global food demand and the sustainable
145 intensification of agriculture. P Natl Acad Sci USA, 108(50): 20260-20264.

146 Travasso, M.I., Magrin, G.O., Rodriguez, R. and Grondona, M.O., 1995. Comparing CERES-
147 Wheat and SUCROS2 in the Argentinean Cereal Region. In: A. Zerger and R.M. Argent
148 (Editors), Internationa Congress on Modelling and Simulation. Modelling and Simulation
149 Society of Australia and New Zealand, The University of Newcastle, Newcastle, NSW,
150 pp. 366-369.

151 Tubiello, F.N. et al., 2007. Crop response to elevated CO2 and world food supply - A comment
152 on "Food for Thought..." by Long et al., Science 312 : 1918-1921, 2006. Eur J Agron,
153 26(3): 215-223.

154 Tubiello, F.N. and Ewert, F., 2002. Simulating the effects of elevated CO2 on crops: approaches
155 and applications for climate change. European Journal of Agronomy, 18(1-2): 57-74.

156 Utset, A., Farre, I., Martinez-Cob, A. and Cavero, J., 2004. Comparing Penman-Monteith and
157 Priestley-Taylor approaches as reference-evapotranspiration inputs for modeling maize
158 water-use under Mediterranean conditions. Agricultural Water Management, 66(3): 205-
159 219.

160 Wang, L., Feng, Z.Z. and Schjoerring, J.K., 2013. Effects of elevated atmospheric CO2 on
161 physiology and yield of wheat (Triticum aestivum L.): A meta-analytic test of current
162 hypotheses. Agr Ecosyst Environ, 178: 57-63.

163 White, J.W., Hoogenboom, G., Kimball, B.A. and Wall, G.W., 2011a. Methodologies for
164 simulating impacts of climate change on crop production. Field Crop Res, 124(3): 357-
165 368.

166 White, J.W., Hoogenboom, G., Wilkens, P.W., Stackhouse, P.W. and Hoel, J.M., 2011b.
167 Evaluation of Satellite-Based, Modeled-Derived Daily Solar Radiation Data for the
168 Continental United States. Agron J, 103(4): 1242-1251.

169 Wu, L. and Kersebaum, K.C., 2008. Modeling water and nitrogen interaction responses and their
170 consequences in crop models. In: L.R. Ahuja, V.R. Reddy, S.A. Saseendran and Q. Yu
171 (Editors), Response of crops to limited water: understanding and modeling water stress
172 effects on plant growth processes. Advances in Agricultural Systems Modeling. ASA,
173 CSSA, SSSA, Madison, WI, USA, pp. 215-249.

174 Xu, C.Y. and Singh, V.P., 2002. Cross comparison of empirical equations for calculating
175 potential evapotranspiration with data from Switzerland. Water Resources Management,
176 16(3): 197-219.

177

Table 1. Average (AV), standard deviation (STD), and coefficient of variability (CV%) for the Netherlands (NL), Argentina (AR), India (IN), and Australia (AU) for seven parameters using the 16 crop simulation models.

Variable	Unit	AV	STD	CV%	AV	STD	CV%	AV	STD	CV%	AV	STD	CV%
1-Year			**NL**			**AR**			**IN**			**AU**	
ET0[a]	*(mm)*	548.8	92.7	16.9	516.7	56.4	10.9	590.1	92.6	15.7	647.2	68.4	10.6
WU[b]	*(mm)*	445.4	100.3	22.5	371.3	51.7	13.9	301.9	49.9	16.5	234	38.4	16.4
T_a[c]	*(mm)*	301.7	85.7	28.4	271.6	53.9	19.8	232.5	66.3	28.5	132.1	43.8	33.2
E_s[d]	*(mm)*	143.7	60.6	42.2	99.6	33.4	33.5	69.4	50.7	73.1	101.9	39.8	39.1
Yield	*(t ha^{-1})*	7.7	0.4	5.7	6.1	0.5	9	4	0.4	10.4	2.2	0.5	21.9
WUE[e]	*(kg ha^{-1} mm^{-1})*	18.1	4.1	22.6	16.6	2.6	15.6	13.8	2.6	19	9.9	3.7	37.3
T_{eff}[f]	*(kg ha^{-1} mm^{-1})*	29.2	16	55	23.3	5.6	24	19.3	7.4	38.4	18.9	8.2	43.2
Baseline (30-years)													
ET0	*(mm)*	556.7	88.3	15.9	539.6	55.4	10.3	564.6	68.7	12.2	692.7	68.8	9.9
WU	*(mm)*	449.9	99.3	22.1	365.9	58.9	16.1	329.4	52	15.8	258.6	49.7	19.2
T_a	*(mm)*	297.9	75.3	25.3	257	50.1	19.5	244.8	62.9	25.7	154.4	46.9	30.4
E_s	*(mm)*	152	56.9	37.5	109	35.9	33	84.7	46.7	55.1	104.2	44.2	42.4
Yield	*(t ha^{-1})*	7.4	0.9	12.3	5.5	0.4	8	5	0.6	12.2	2.8	0.6	21.4
WUE	*(kg ha^{-1} mm^{-1})*	17.3	4.9	28.1	15.6	3.2	20.5	15.4	1.8	11.6	11.3	4.2	36.7
T_{eff}	*(kg ha^{-1} mm^{-1})*	27.5	13.4	48.6	22.5	5.8	25.9	21.9	6.7	30.5	20.4	10.1	49.3

[a]Potential evapotranspiration; [b]Water use; [c]Crop transpiration; [d]Soil evaporation; [e]Water use efficiency; [f]Transpiration efficiency.

Figure Caption

Figure 1. Simulated potential reference evapotranspiration (ET_0) and percentage of simulated water use variance. (*a*) Simulated seasonal ET_0 for the 30-year baseline calculated from the average of those models using Penman-Monteith (PM, 7 models), Priestley-Taylor (PT, 6 models), and Penman (P, 3 models) equations. Different letters indicate significant differences at $\alpha = 0.05$. (*b*-d) Simulated proportion of variance for water use explained by ET_0 (light grey), crop transpiration (*Ta*; black), and soil evaporation (*Es*; white) for (*b*) the experimental year and the 30-year baseline, (*c*) average daily air temperature increases, and (*d*) increasing atmospheric CO_2 concentrations.

Figure 2. Daily variability in plant water use and crop growth-related variables for an experimental site in the Netherlands (NL). (*a*) Daily growing season rainfall. (*b*-*h*) Average of 16 crop models (black line) with the interval between the 20th and 80th percentiles (shaded grey area) for plant available water (PAW), daily potential evapotranspiration (ET0), leaf area index (LAI), soil evaporation (Es), plant transpiration (Ta), water use (WU), and aboveground biomass (AGB). Observed values (closed symbols) are shown for plant available soil water, LAI, and above-ground biomass.

Figure 3. Daily variability in plant water use and crop growth-related variables for an experimental site in Argentina (AR). (*a*) Daily growing season rainfall. (*b*-*h*) Average of 16 crop models (black line) with the interval between the 20th and 80th percentiles (shaded grey area) for plant available water (PAW), daily potential evapotranspiration (ET0), leaf area index (LAI), soil evaporation (Es), plant transpiration (Ta), water use (WU), and aboveground biomass (AGB). Observed values (closed symbols) are shown for plant available soil water, LAI, and above-ground biomass.

Figure 4. Daily variability in plant water use and crop growth-related variables for an experimental site in India (IN). (*a*) Irrigation. (*b*-*h*) Average of 16 crop models (black line) with the interval between the 20th and 80th percentiles (shaded grey area) for plant available water (PAW), daily potential evapotranspiration (ET0), leaf area index (LAI), soil evaporation (Es), plant transpiration (Ta), water use (WU), and aboveground biomass (AGB). Observed values (closed symbols) are shown for plant available soil water, LAI, water use, and above-ground biomass.

Figure 5. Daily variability in plant water use and crop growth-related variables for an experimental site in Australia (AU). (*a*) Daily growing season rainfall. (*b-h*) Average of 16 crop models (black line) with the interval between the 20th and 80th percentiles (shaded grey area) for plant available water (PAW), daily potential evapotranspiration (ET0), leaf area index (LAI), soil evaporation (Es), plant transpiration (Ta), water use (WU), and aboveground biomass (AGB). Observed values (closed symbols) are shown for plant available soil water, water use, and above-ground biomass.

Figure 6. Effects of higher temperatures, respect to the 30 years historical data, on simulated water use related variables and grain yield. Boxplot of the relative change of multi-model simulations with increases in average daily air temperature of 3°C and 6°C for water use (WU), grain yield (*Y*), cumulative crop transpiration (*Ta*), cumulative soil evaporation (*Es*), water use efficiency (WUE), and transpiration efficiency (T_{eff}), for experimental sites in the Netherlands (NL), Argentina (AR), India (IN), and Australia (AU). The percentage of individual models that predict the same trend is shown above each set of points.

Figure 7. Effects of increases in atmospheric CO_2 concentrations on simulated water use related variables and grain yield. Boxplot of the relative change of multi-model simulation with increased atmospheric CO_2 concentrations for water use (WU), grain yield (*Y*), cumulative crop transpiration (*Ta*), cumulative soil evaporation (*Es*), water use efficiency (WUE), and transpiration efficiency (T_{eff}), for experiment sites in the Netherlands (NL), Argentina (AR), India (IN), and Australia (AU). The percentage of individual models that predict the same trend as the multi-model mean is shown above each set of points.

Figure 8. Interaction patterns between temperature and atmospheric CO_2 concentration on simulated water use related variables and grain yield. Relative change in (*a, f, k,* and *p*) water use (WU), (*b, g, l,* and *q*) grain yield (*Y*), (*c, h, m,* and r) cumulative crop transpiration (*Ta*), (d*, i, n,* and *s*) water use efficiency (WUE), and (*e, j, o,* and *t*) transpiration efficiency (T_{eff}) simulations for experimental sites in (a-e) the Netherlands, (*f*-j) Argentina, (*k*-o) India, and Australia (*p*-t) with increases in average daily air temperature versus atmospheric CO_2 concentration.

Figure 9. Boxplots of the simulated Soil Water Balance (SWB) calculated using eq. [2] for the Netherlands (NL), Argentina (AR), India (IN), and Australia (AU); (*a*) Effect of temperature on each of the model simulation of the baseline 30-years period (Base), the increases in average

daily air temperature of 3°C (T3) and 6°C (T6); (*b*) for the increases in atmospheric CO_2 concentrations.

Figure 10. Boxplots of the simulated components of the Soil Water Balance (SWB) calculated using eq. [2]. Simulated Drainage (*Drain*), Runoff (*Runoff*), crop transpiration (*Ta*), and soil evaporation (*Es*) are shown for the Netherlands (NL), Argentina (AR), India (IN), and Australia (AU); (*a*) Effect of temperature on each of the model simulation of the baseline 30-years period (Base), the increases in average daily air temperature of 3°C (T3) and 6°C (T6); (*b*) for the increases in atmospheric CO_2 concentrations.

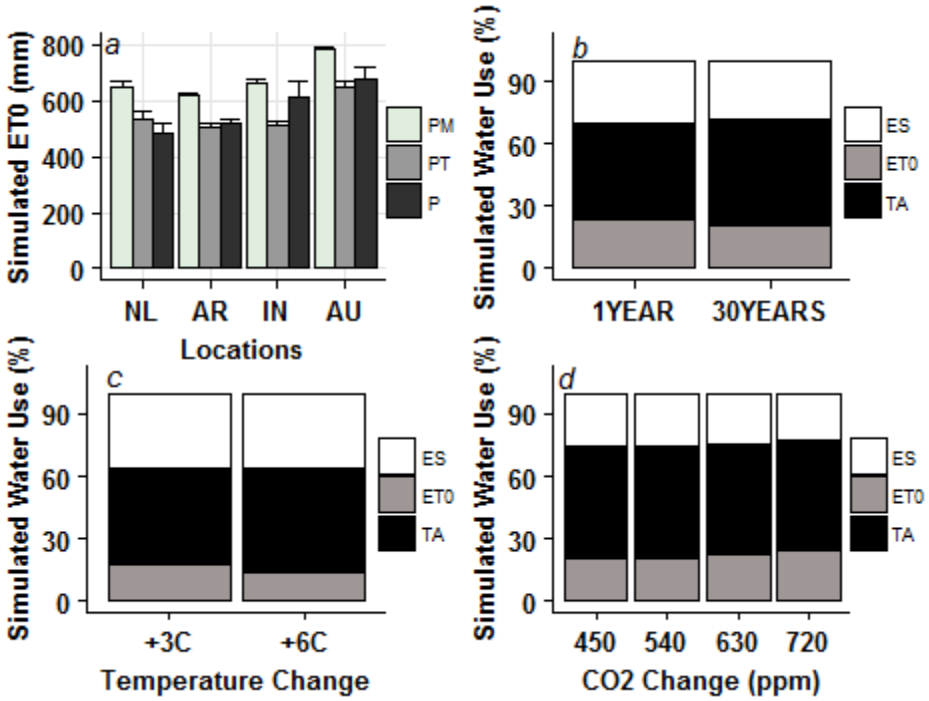
a
Simulated ET0 (mm)
800
600
400
200
0
NL
AR
IN
AU
Locations
PM
PT
P
b
Simulated Water Use (%)
90
60
30
0
1YEAR
30YEARS
ES
ET0
TA
c
Simulated Water Use (%)
+3C
+6C
Temperature Change
d
450
540
630
720
CO2 Change (ppm)

Figure 1.

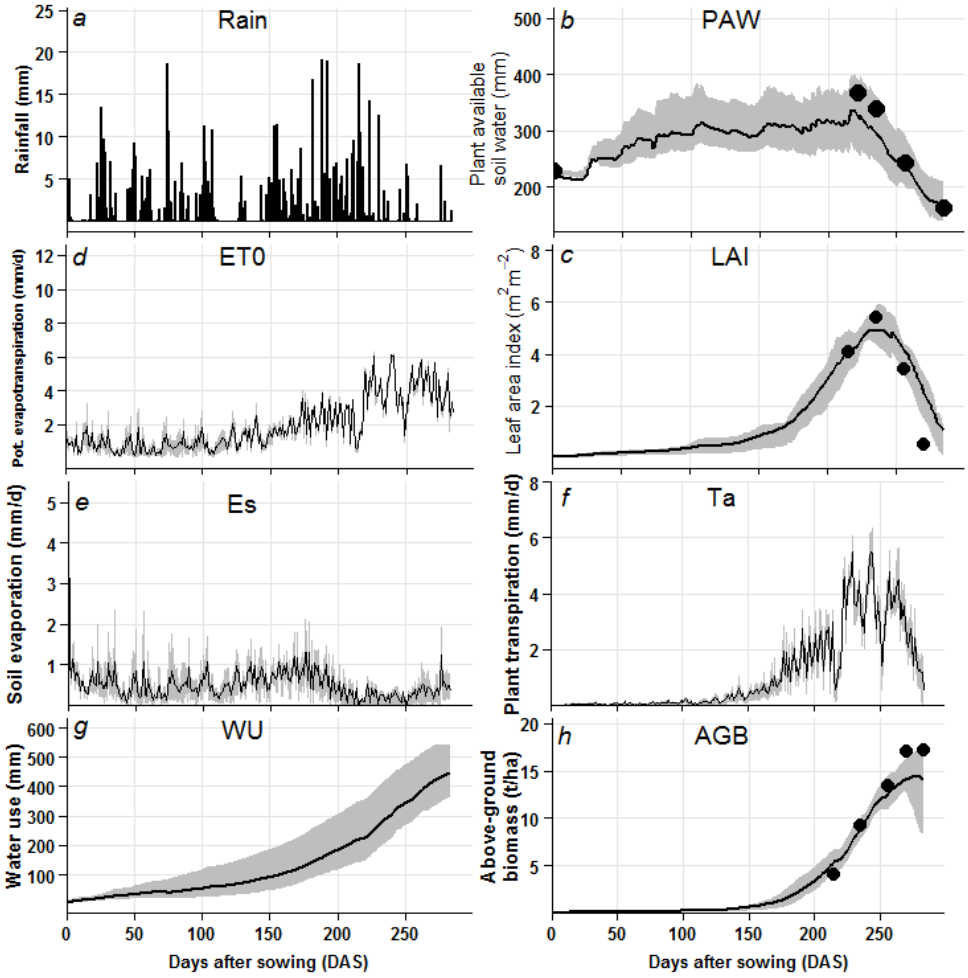
a
Rain
Rainfall (mm)
b
PAW
Plant available soil water (mm)
d
ET0
Pot. evapotranspiration (mm/d)
c
LAI
Leaf area index (m2 m−2)
e
Es
Soil evaporation (mm/d)
f
Ta
Plant transpiration (mm/d)
g
WU
Water use (mm)
h
AGB
Above-ground biomass (t/ha)
Days after sowing (DAS)
Days after sowing (DAS)

Figure 2.

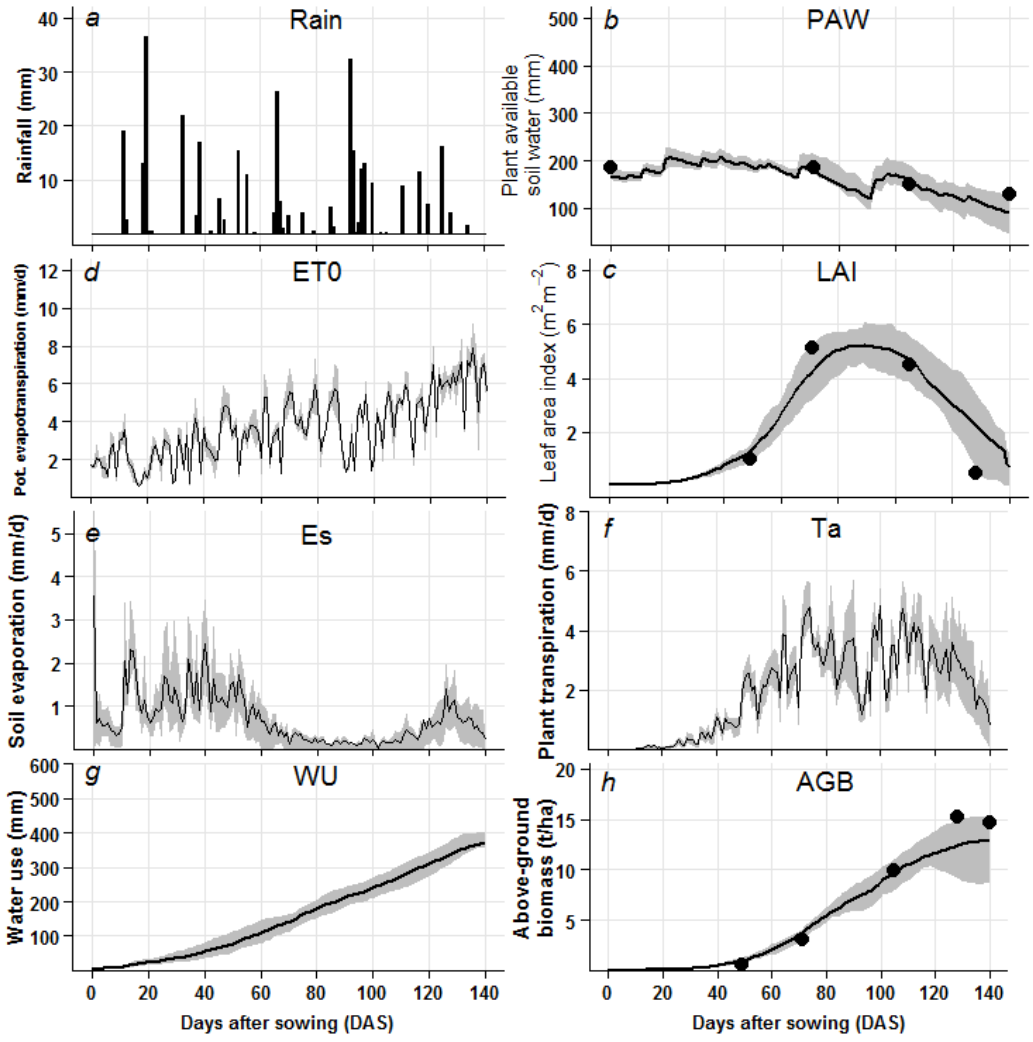
a
Rain
Rainfall (mm)
b
PAW
Plant available soil water (mm)
d
ET0
Pot. evapotranspiration (mm/d)
c
LAI
Leaf area index (m2 m-2)
e
Es
Soil evaporation (mm/d)
f
Ta
Plant transpiration (mm/d)
g
WU
Water use (mm)
h
AGB
Above-ground biomass (t/ha)
Days after sowing (DAS)
Days after sowing (DAS)

Figure 3.

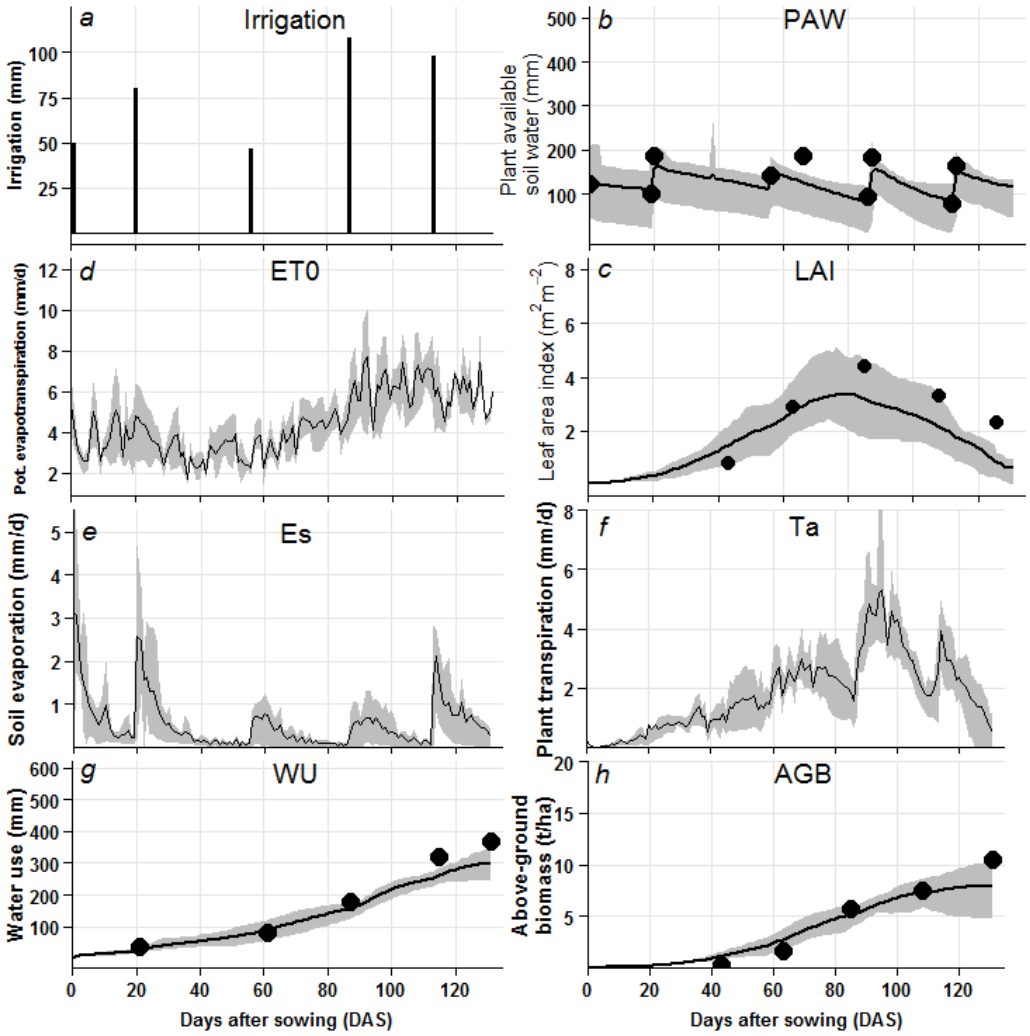
a
Irrigation
Irrigation (mm)
b
PAW
Plant available soil water (mm)
d
ET0
Pot. evapotranspiration (mm/d)
c
LAI
Leaf area index (m2 m−2)
e
Es
Soil evaporation (mm/d)
f
Ta
Plant transpiration (mm/d)
g
WU
Water use (mm)
h
AGB
Above-ground biomass (t/ha)
Days after sowing (DAS)
Days after sowing (DAS)

Figure 4.

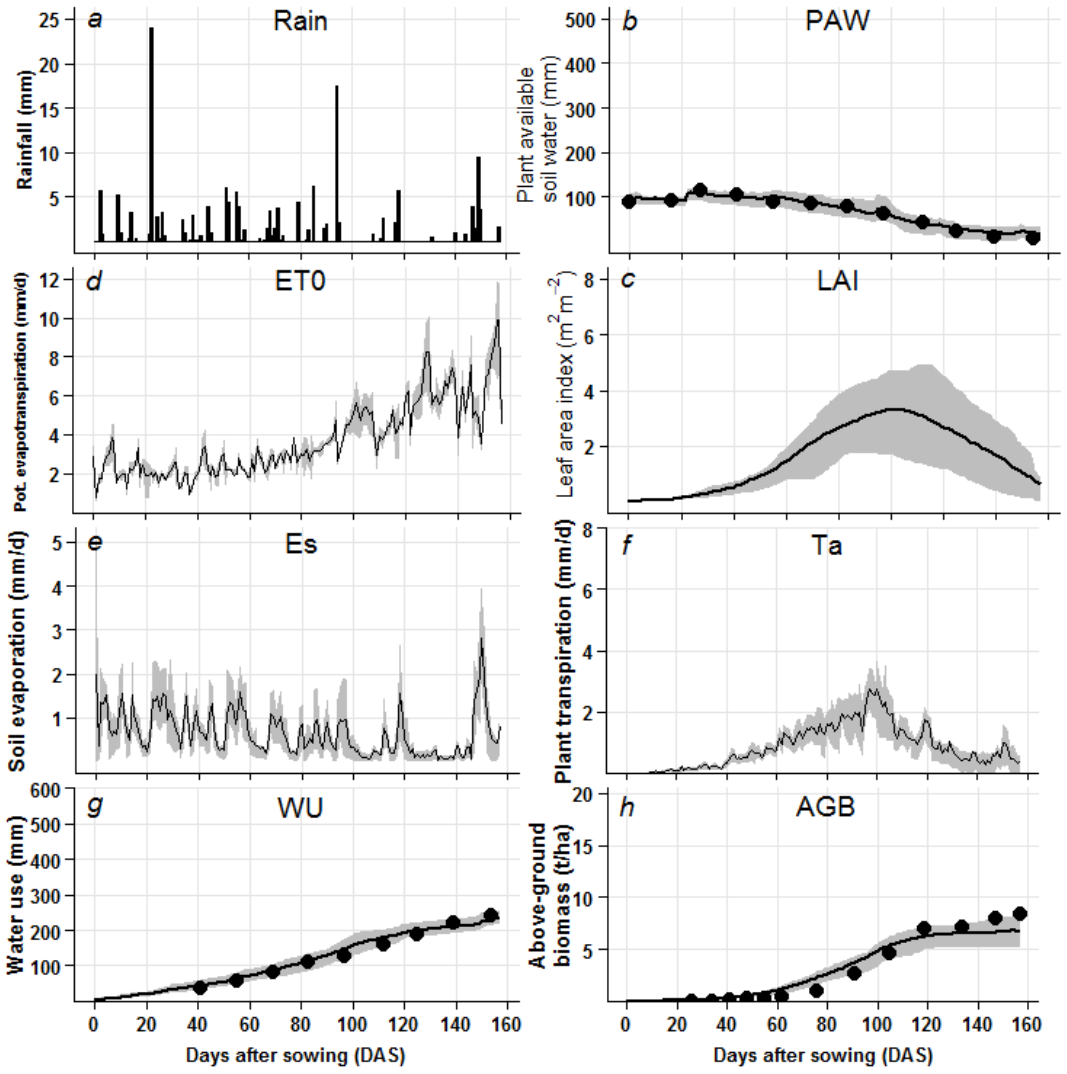
a
Rain
Rainfall (mm)
b
PAW
Plant available soil water (mm)
d
ET0
Pot. evapotranspiration (mm/d)
c
LAI
Leaf area index (m²m⁻²)
e
Es
Soil evaporation (mm/d)
f
Ta
Plant transpiration (mm/d)
g
WU
Water use (mm)
h
AGB
Above-ground biomass (t/ha)
Days after sowing (DAS)
Days after sowing (DAS)

Figure 5.

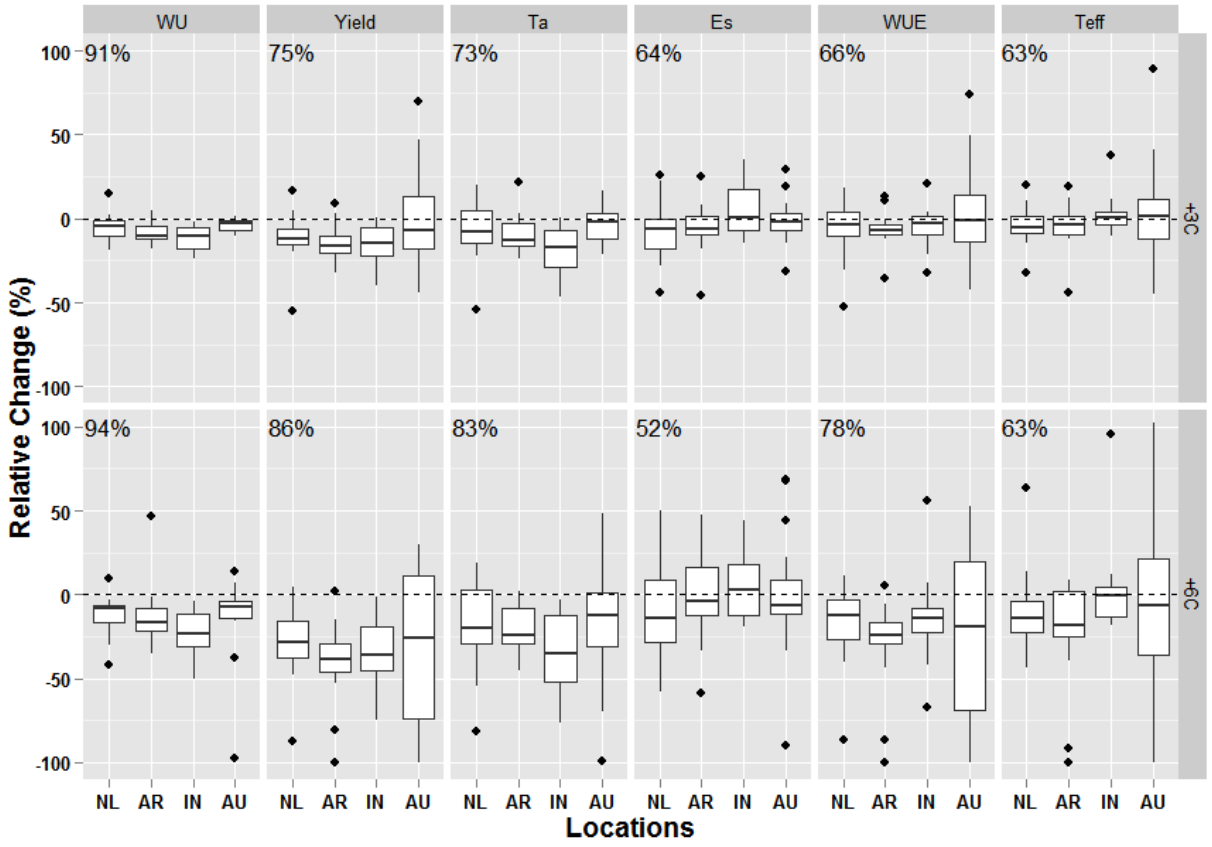
WU
Yield
Ta
Es
WUE
Teff
91%
75%
73%
64%
66%
63%
94%
86%
83%
52%
78%
63%
+3C
+6C
Relative Change (%)
100
50
0
-50
-100
NL
AR
IN
AU
Locations

Figure 6.

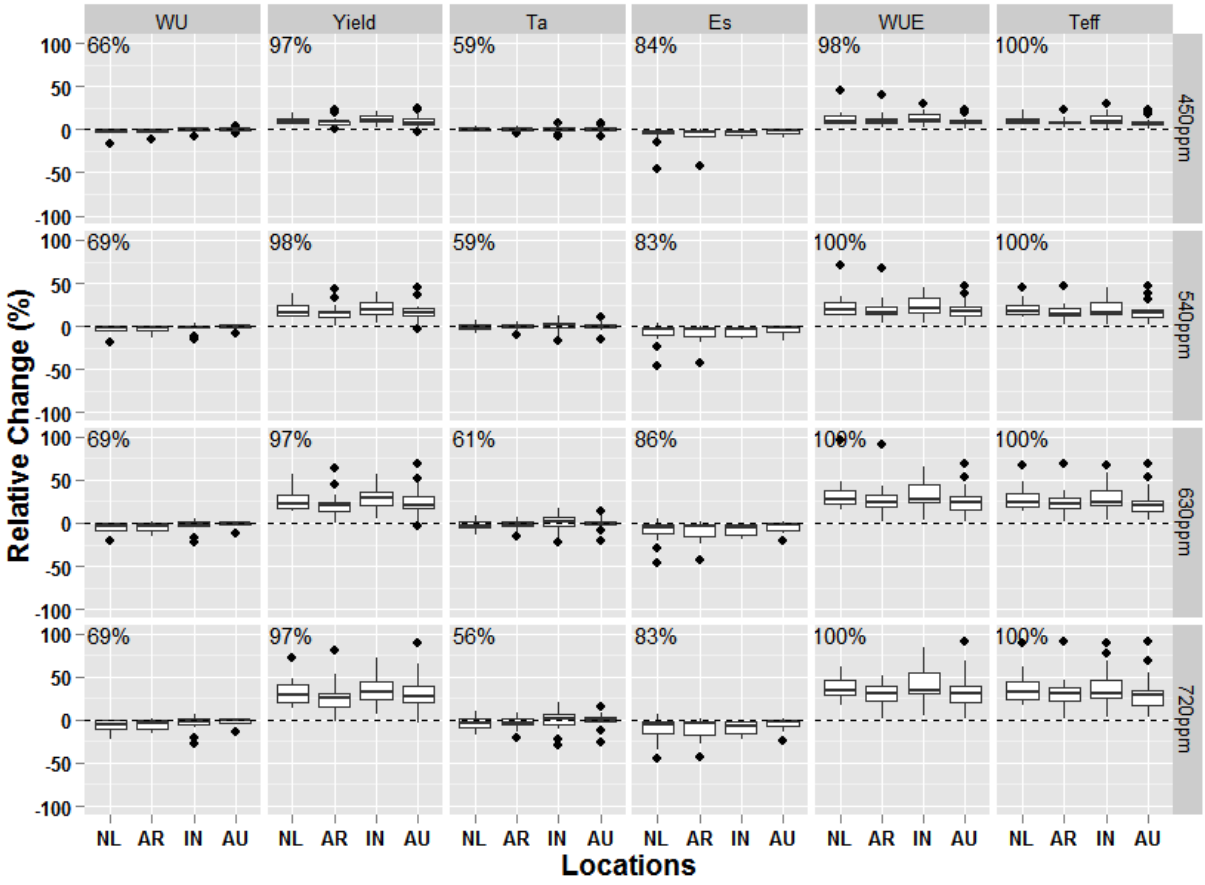
WU
Yield
Ta
Es
WUE
Teff
450ppm
540ppm
630ppm
720ppm
66%
97%
59%
84%
98%
100%
69%
98%
59%
83%
100%
100%
69%
97%
61%
86%
100%
100%
69%
97%
56%
83%
100%
100%
Relative Change (%)
100
50
0
-50
-100
NL
AR
IN
AU
Locations

Figure 7.

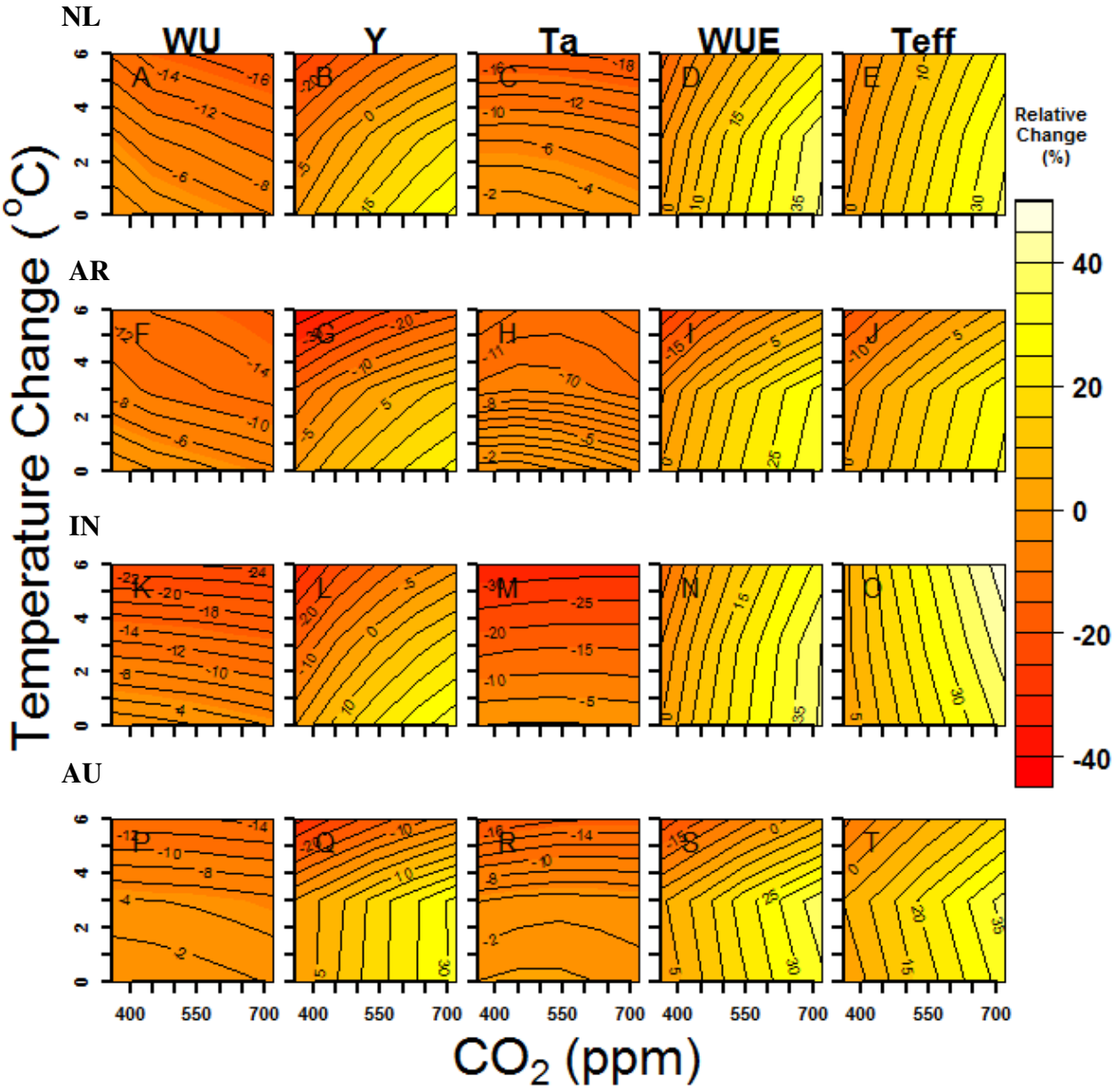
NL
AR
IN
AU
WU
Y
Ta
WUE
Teff
A
B
C
D
E
F
G
H
I
J
K
L
M
N
O
P
Q
R
S
T
Temperature Change (°C)
CO2 (ppm)
Relative Change (%)
40
20
0
-20
-40
400
550
700

Figure 8.

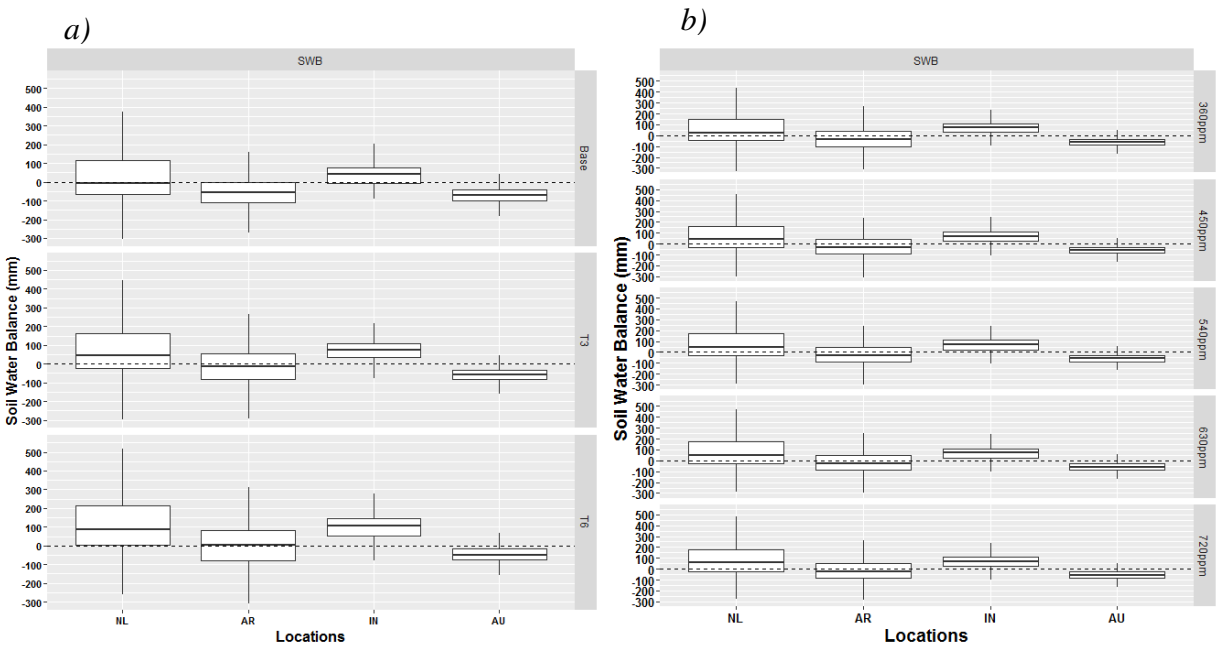
a)
b)
SWB
Base
T3
T6
360ppm
450ppm
540ppm
630ppm
720ppm
Soil Water Balance (mm)
NL
AR
IN
AU
Locations

Figure 9.

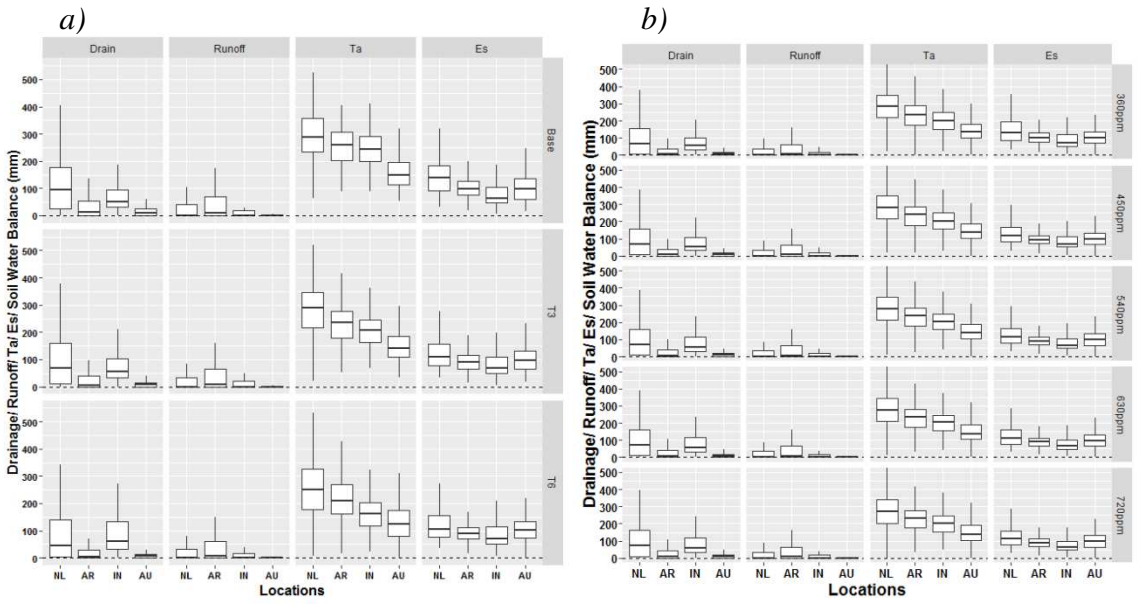
a)
b)
Drain
Runoff
Ta
Es
Base
T3
T6
360ppm
450ppm
540ppm
630ppm
720ppm
Drainage/ Runoff/ Ta/ Es/ Soil Water Balance (mm)
Locations
NL
AR
IN
AU

Figure 10.

SUPPLEMENTAL INFORMATION

Table S1. Field experiments, crop management and climate characteristics of the four sites where models were calibrated modified after Asseng et al. (2013).

	Experiment			
Location	Wageningen	Balcarce	New Delhi	Wongan Hills
Country	The Netherlands	Argentina	India	Australia
Latitude[a]	51.97	-37.5	28.38	-30.89
Longitude[a]	5.63	-58.3	77.12	116.72
Environment	High-yielding long-season	High/medium-yielding medium-season	Irrigated short-season	Low-yielding rain-fed short-season
	Soils			
Soil type	Silty clay loam	Clay loam	Sandy loam	Loamy sand
Maximum root depth (cm)	200	130	160	210
Plant available soil water content (mm to maximum rooting depth)	354	205	121	125
	Crop management			
Cultivar	Arminda	Oasis	HD 2009	Gamenya
Sowing date (day of year)	294	223	328	164
Total applied N fertilizer (kg N ha^{-1})	160	120	120	50
Total irrigation (mm)	0	0	383	0
	Phenology			
Anthesis (day of year)	178	328	49	275
Maturity (day of year)	213	363	93	321
Growing Season Length (days)	284	140	130	157
	Environmental Characteristics			
Experimental year	1982/1983	1992	1984/1985	1984
Mean growing season air temperature (°C)	8.8	13.7	17.3	14.0
Mean growing season rainfall (mm)	595	336	0	164
30 years average	1981-2010	1981-2010	1981-2010	1981-2010
Mean growing season air temperature (°C)	8.5	12.0	18.9	16.2
Mean growing season rainfall (mm)	716	395	84	246

[a]Geographical degrees and minutes – the latter expressed in decimals; the minus sign before latitude and longitude indicates South of equator and West of Greenwich (0) meridian.

Table S2. Soil depth, hydraulic limits, bulk density, organic carbon, and soil pH provided to the modelling group for each site.

Location	Depth (cm)	LL (cm3 cm^{-3})	DUL (cm3 cm^{-3})	SAT (cm3 cm^{-3})	BD (g cm^{-3})	OC (%)	pH
the Netherlands	5	0.18	0.39	0.49	1.35	2.80	6
	10	0.18	0.39	0.49	1.35	2.80	6
	20	0.18	0.39	0.49	1.35	2.80	6
	30	0.18	0.39	0.49	1.35	2.80	6
	40	0.18	0.37	0.49	1.35	1.40	6
	60	0.20	0.37	0.49	1.35	1.40	6
	80	0.20	0.37	0.49	1.35	1.20	6
	100	0.20	0.37	0.49	1.35	1.20	6
	130	0.20	0.37	0.49	1.35	1.00	6
	200	0.20	0.37	0.49	1.35	1.00	6
Argentina	5	0.16	0.38	0.47	1.05	3.15	6.2
	20	0.17	0.35	0.45	1.10	3.30	5.9
	40	0.18	0.36	0.43	1.15	1.20	6.0
	60	0.18	0.38	0.48	1.30	0.70	6.4
	80	0.26	0.40	0.49	1.35	0.30	6.6
	100	0.14	0.30	0.40	1.30	0.10	6.5
	120	0.14	0.30	0.40	1.30	0.10	6.5
India	15	0.11	0.17	0.37	1.56	0.45	7.9
	30	0.11	0.17	0.37	1.59	0.35	8.0
	60	0.11	0.18	0.37	1.50	0.31	8.0
	90	0.11	0.18	0.37	1.50	0.20	8.2
	120	0.12	0.19	0.37	1.55	0.19	8.5
	150	0.12	0.19	0.37	1.54	0.19	8.6
	180	0.12	0.19	0.37	1.58	0.19	8.6
Australia	5	0.07	0.13	0.35	1.31	1.23	4.70
	10	0.07	0.13	0.35	1.31	0.43	5.10
	20	0.08	0.14	0.35	1.45	0.37	5.10
	30	0.09	0.14	0.35	1.48	0.26	6.00
	40	0.09	0.15	0.35	1.51	0.24	6.00
	50	0.09	0.15	0.35	1.53	0.21	6.00
	70	0.09	0.15	0.35	1.50	0.20	6.00
	90	0.10	0.16	0.35	1.50	0.19	6.00
	120	0.10	0.16	0.35	1.50	0.18	6.00
	150	0.11	0.18	0.35	1.50	0.18	6.00
	180	0.12	0.18	0.35	1.50	0.18	6.00
	210	0.13	0.18	0.35	1.50	0.17	6.00

Table S3. Modeling approaches of 26 wheat simulation models used in this study, modified after Asseng et al. (2013).

Model	Leaf area / light interception [a]	Light utilization [b]	Yield formation [c]	Phenology [d]	Root distribution over depth [e]	Environmental constraints involved [f]	Type of water stress [g]	Type of heat stress [h]	Water dynamics [i]	Evapotranspiration [j]	Soil CN-model [k]	Process modified by elevated CO_2 [l]	No. cultivar parameters	Climate input variables [m]	Model relative [n]	Model type [o]
APSIM-Nwheat	S	RUE	Prt	T/DL/V	EXP	W/N/A	S	V	C	PT	CN/P(3)/B	RUE/TE	7	R/Tx/Tn/Rd	C	P
APSIM-wheat	S	RUE	Prt/Gn/B	T/DL/V/O	O	W/N/A	E	-	C/R	**PT**/PM	CN/P(3)/B	RUE/TE /CLN	7	R/Tx/Tn/Rd/e/W	C	P
AquaCrop	S	TE	HI/B	T/DL/V/O	EXP	W/N/H	E/S	V/R	C	FAO PM	none	TE	2	R/Tx/ETo	none	P
CropSyst	S	TE/RUE	HI/B	T/DL/V	EXP	W/N/H	E	R	C/R	PM	N/P(4)	TE/RUE	16	R/Tx/Tn/Rd/RH/W	none	P
DSSAT-CROPSIM-CERES	S	RUE	B/Gn	T/DL/V	EXP	W/N	E/S	-	C	PT	CN/P(4)/B	RUE/TE	7	R/Tx/Tn/Rd/RH/W	C	P
DSSAT-CROPSIM	S	RUE	Prt	T/DL/V	LIN	W/N	E/S	V	C	PT	CN/P(4)/B	RUE/TE	21	R/Tx/Tn/Rd/	none	p
EPIC wheat	S	RUE	HI	T/V	EXP	W/N/H	E	V	C	P/**PM**/PT/HAR	N/P(5)/B	RUE/TE /GY	16	R/Tx/Tn/Rd/RH/W	E	P
Expert-N – CERES	S	RUE	B/Gn	T/DL/V	EXP	W/N	E/S	-	R	PM	CN/P(3)/B	RUE	7	R/Tx/Tn/Rd/RH/W	C	P
Expert-N – GECROS	D	P-R/TE	Gn/Prt	T/DL/V	EXP	W/N	E/S	-	R	PM	CN/P(3)/B	RUE/TE	10	R/Tx/Tn/Rd/RH/W	S	P
Expert-N – SPASS	D	P-R	Gn/Prt	T/DL/V	EXP	W/N	E/S	-	R	PM	CN/P(3)/B	RUE	5	R/Tx/Tn/Rd/RH/W	C/S	P
Expert-N – SUCROS	D	P-R	Prt	T	EXP	W/N	E/S	-	R	PM	CN/P(3)/B	RUE	2	R/Tx/Tn/Rd/RH/W	S	P
FASSET	D	RUE	HI/B	T/DL	EXP	W/N	E/S	-	C	MAK	CN/P(6)/B	RUE	14	R/Tx/Tn/Rd	none	P
GLAM-Wheat	S	RUE/TE	B/HI	T/DL/V	LIN	W/H	E	R	C	PT	none	RUE/TE	22	R/Tx/Tn/Td/Ta/e	none	G
HERMES	D	P-R	Prt	T/DL/V/O	EXP	W/N/A	E/S	-	C	**PM**/TW/PT	N/P(2)	RUE/F	6	R/Tx/Tn/Rd/e/RH/W	S/C	P
InfoCrop	D	RUE	Prt/Gn	T/DL	EXP	W/N/H	E	V/R	C	**PM**/PT	CN/P(2)/B	RUE/TE	10	R/Tx/Tn/Rd/W/E	S	P
LINTUL-4	D	RUE	Prt/B	T/DL	LIN	W/N/A	E	-	C	P	N/P(0)/-*	RUE/TE	4	R/Tx/Tn/Rd/e/W	L	P
LINTUL -FAST	D	RUE	Prt	T/DL/V	EXP	W	E		C	P	CN/P(3)	RUE/TE	4	R/Tx/Tn/Rd/RH	L	P
LPJmL	S	P-R	HI_mws/B	T/V	EXP	W	E	-	C	PT	none	F	3	R/Ta/Rd/Cl	E	G
MCWLA-Wheat	S	P-R	HI/B	T/DL/V	EXP	W/T/H	E	V/ R	R	PM	none	F	7	R/Tx/Tn/Rd/e/W	none	G

MONICA	S	RUE	Prt	T/DL/V/O	EXP	W/N/A/H	E	V	C	PM	CN/P(6)/B	F	15	R/Tx/Tn/Rd/RH/W	S/C	P
O'Leary-model	S	TE	Gn/Prt	T/DL	SIG	W/N/H	E/S	V	C	P	N/P(3)/B	TE	18	R/Tx/Tn/Rd/RH/W	none	P

Table A2. Continued

SALUS	S	RUE	Prt/HI	T/DL/V	EXP	W/N/H	E	V	C	PT	CN/P(3)/B (2)	RUE	18	R/Tx/Tn/Rd	C	P
Sirius	D	RUE	B/Prt	T/DL/V	EXP	W/N	E	-	C	P/**PT**	N/P(2)	RUE	14	R/Tx/Tn/Rd/e/W		P
SiriusQuality	D	RUE	B/Prt	T/DL/V	EXP	W/N	S	-	C	P/**PT**	N/P(2)	RUE	14	R/Tx/Tn/Rd/e/W	I	P
STICS	D	RUE	Gn/B	T/DL/V/O	SIG	W/N/H	E/S	V/R	C	P/PT/**SW**	N/P(3)/B	RUE/TE	15	R/Tx/Tn/Rd/e/W	C	P
WOFOST	D	P-R	Prt/B	T/DL	LIN	W/N*	E/S	-	C	P	P(1)	RUE/TE	3	R/Tx/Tn/Rd/e/W	S	G

[a] S, simple approach (e.g. LAI); D, detailed approach (e.g. canopy layers).
[b] RUE, radiation use efficiency approach; P-R, gross photosynthesis – respiration; TE, transpiration efficiency biomass growth.
[c] HI, fixed harvest index; B, total (above-ground) biomass; Gn, number of grains; Prt, partitioning during reproductive stages; HI_mw, harvest index modified by water stress.
[d] T, temperature; DL, photoperiod (day length); V, vernalization; O, other water/nutrient stress effects considered.
[e] LIN, linear, EXP, exponential, SIG, sigmoidal, Call, carbon allocation; O, other approaches.
[f] W, water limitation; N, nitrogen limitation; A, aeration deficit stress; H, heat stress.
[g] E, actual to potential evapotranspiration ratio; S, soil available water in root zone.
[h] V, vegetative organ (source); R, reproductive organ (sink).
[i] C, capacity approach; R, Richards approach.
[j] P, Penman; PM, Penman-Monteith; PT, Priestley –Taylor; TW, Turc-Wendling; MAK, Makkink; HAR, Hargreaves; SW, Shuttleworth and Wallace (resistive model), ("bold" indicates approached used during the study).
[k] CN, CN model; N, N model; P(x), x number of organic matter pools; B, microbial biomass pool.
[l] RUE, radiation use efficiency; TE, transpiration efficiency; GY, grain yield; CLN, critical leaf N concentration; F, Farquhar model.
[m] Cl, cloudiness; R, rainfall; Tx, maximum daily temperature; Tn, minimum daily temperature; Ta, average daily temperature; Td, dew point temperature; Rd, radiation; e, vapor pressure; RH, relative humidity; W, wind speed.
[n] C, CERES; L, LINTUL; E, EPIC; S, SUCROS; I, Sirius.
[o] P, point model; G, global or regional model (regarding the main purpose of model).
[*] nitrogen-limited yields can be calculated for given soil nitrogen supply and N fertilizer applied, but model has no N simulation routines.